ЖЭТФ, 2004, том 126, вып. 3 (9), стр. 642–649

PARAMETERS OF THE EFFECTIVE SINGLET–TRIPLET MODEL FOR BAND STRUCTURE OF HIGH-T_c CUPRATES BY VARIOUS APPROACHES

*M. M. Korshunov**, *V. A. Gavrichkov*, *S. G. Ovchinnikov*

Kirensky Institute of Physics, Siberian Branch of Russian Academy of Sciences
660036, Krasnoyarsk, Russia

Z. V. Pchelkina, *I. A. Nekrasov*, *M. A. Korotin*, *V. I. Anisimov*

Institute of Metal Physics, Ural Branch of Russian Academy of Sciences
620219, Ekaterinburg GSP-170, Russia

Submitted 2 December 2003

We consider the problem of determining the parameters for high-T_c superconducting copper oxides. Various approaches, the *ab initio* LDA and LDA + U calculations and the generalized tight-binding (GTB) method for strongly correlated electron systems, are used to calculate hopping and exchange parameters of the effective singlet–triplet model for the CuO_2 layer. The resulting parameters are in remarkably good agreement with each other and with parameters extracted from experiment. This set of parameters is proposed for proper quantitative description of physics of hole-doped high-T_c cuprates in the framework of effective models.

PACS: 74.72.h, 74.20.z, 74.25.Jb, 31.15.Ar

1. INTRODUCTION

High-T_c superconducting cuprates (HTSC) belong to the class of substances where strong electron correlations are important. This circumstance and also the fact that these substances have nontrivial phase diagrams (see, e.g., reviews [1]) complicate the description of HTSC in the framework of first-principle (*ab initio*) methods, especially in the low doping region. Therefore, the most adequate method of theoretical investigations of HTSC is currently the model approach. Effective models of HTSC (e.g., the t–J model) usually contain free parameters that could be fitted to experimental data (comparison of the calculated and experimental Fermi surfaces, dispersion curves, etc.), but the question concerning correctness of these parameters arises in the model approach. One of the possible ways to answer this question is to obtain relations between parameters of some effective model and microscopic parameters of the underlying crystal structure. The underlying crystal structure of HTSC can be described either by the 3-band Emery model [2, 3] or by the multiband p–d model [4]. One can compare the parameters in these models with the parameters obtained by very different approach, e.g., with *ab initio* calculated parameters. This does not mean that the *ab initio* band structure is correct. Due to strong electron correlations, it is certainly incorrect in the low doping region, where these correlations are most significant. Nevertheless, the single electron parameters are of interest and may be compared with the appropriate parameters obtained by fitting to the experimental ARPES data.

In the present paper, we obtain relations between microscopic parameters of the multiband p–d model and parameters of the effective singlet–triplet t–J model for hole-doped HTSC. We then compare these parameters and the t–J model parameters obtained in the *ab initio* calculations. In Sec. 2, the details of *ab initio* calculations within the density functional theory are presented. In Sec. 3, the effective singlet–triplet model is formulated as the low-energy Hamiltonian for the multiband p–d model with the generalized tight-binding (GTB) method applied. In both methods, the parent insulating compound La_2CuO_4 is investigated.

*E-mail: mkor@iph.krasn.ru

The parameters are obtained at zero doping, because within the GTB method, the evolution of the band structure with doping is described only by changes in the occupation numbers of zero-hole, single-hole, and two-hole local terms, while all the parameters are fitted in the undoped case and are therefore fixed for all doping levels. The resulting parameters of both approaches (GTB and *ab initio*) are in very good qualitative and quantitative agreement with each other and with the parameters extracted from experiment. Also, these parameters are in reasonable agreement with the t–J model parameters used in the literature. We conclude that the obtained set of model parameters should be used in effective models for proper quantitative description of HTSC in the whole doping region.

2. *AB INITIO* CALCULATION OF PARAMETERS

The band structure of La_2CuO_4 was obtained in the framework of the linear muffin-tin orbital method [5] in the tight-binding approach [6] (TB-LMTO) within the local density approximation (LDA). The crystal structure data [7] corresponds to tetragonal La_2CuO_4. The effective hopping parameters t_ρ were calculated by the least square fit procedure to the bands obtained in the LDA calculation [8]. The effective exchange interaction parameters J_ρ were calculated using the formula derived in [9], where the Green's function method was used to calculate J_ρ as the second derivative of the ground state energy with respect to the magnetic moment rotation angle via eigenvalues and eigenfunctions obtained in the LDA + U calculation [10]. The LDA + U approach allows obtaining the experimental antiferromagnetic insulating ground state for the undoped cuprate: in contrast, the LDA approach gives a nonmagnetic metallic ground state [10]. The Coulomb parameters $U = 10$ eV and $J = 1$ eV used in the LDA + U calculation were obtained in constrained LSDA supercell calculations [11].

3. GTB METHOD AND FORMULATION OF THE EFFECTIVE SINGLET–TRIPLET MODEL

The t–J [12] and Hubbard [13] models are widely used to investigate HTSC compounds. In using these models, one can in principle describe qualitatively essential physics. The parameters in these models (i.e., the hopping integral t, antifferomagnetic exchange J, and Hubbard repulsion U) are typically extracted from experimental data. Therefore, these parameters do not have a direct microscopical meaning. A more systematic approach is to write the multiband Hamiltonian for the real crystal structure (which now includes parameters of this *real* structure) and map this Hamiltonian onto some low-energy model (like the t–J model). In this case, parameters of the real structure could be taken from the *ab initio* calculations or fitted to experimental data.

It is convenient to use the 3-band Emery p–d model [2, 3] or the multiband p–d model [4] as the starting model that properly describes crystal structure of the cuprates. The set of microscopic parameters for the first model was calculated in [14, 15]. While this model is simplier than the multiband p–d model, it lacks some significant features, namely the importance of d_{z^2} orbitals on copper and p_z orbitals on apical oxygen. Nonzero occupancy of d_{z^2} orbitals was pointed out in XAS and EELS experiments, which show 2–10 % occupancy of d_{z^2} orbitals [16, 17] and 15 % doping-dependent occupancy of p_z orbitals [18] in all HTSC of the p-type (hole doped). In order to take these facts into account, the multiband p–d model should be used,

$$H_{pd} = \sum_{f,\lambda,\sigma} (\epsilon_\lambda - \mu) n_{f\lambda\sigma} + \sum_{\langle f,g\rangle} \sum_{\lambda,\lambda',\sigma} T_{fg}^{\lambda\lambda'} c_{f\lambda\sigma}^{+} c_{g\lambda'\sigma} +$$

$$+ \frac{1}{2} \sum_{f,g,\lambda,\lambda'} \sum_{\sigma_1,\sigma_2,\sigma_3,\sigma_4} V_{fg}^{\lambda\lambda'} c_{f\lambda\sigma_1}^{+} c_{f\lambda\sigma_3} c_{g\lambda'\sigma_2}^{+} c_{g\lambda'\sigma_4}, \quad (1)$$

where $c_{f\lambda\sigma}$ is the annihilation operator in the Wannier representation of the hole at site f (copper or oxygen) at orbital λ with spin σ, and $n_{f\lambda\sigma} = c_{f\lambda\sigma}^{+} c_{f\lambda\sigma}$. The indices λ run through $d_{x^2-y^2} \equiv d_x$ and $d_{3z^2-r^2} \equiv d_z$ orbitals on copper, p_x and p_y atomic orbitals on plane oxygen sites, and p_z orbital on apical oxygen; ϵ_λ is the single-electron energy of the atomic orbital λ; $T_{fg}^{\lambda\lambda'}$ includes hopping matrix elements between copper and oxygen (t_{pd} for hopping $d_x \leftrightarrow p_x, p_y$; $t_{pd}/\sqrt{3}$ for $d_z \leftrightarrow p_x, p_y$; t'_{pd} for $d_z \leftrightarrow p_z$) and between oxygen and oxygen (t_{pp} for hopping $p_x \leftrightarrow p_y$; t'_{pp} for hopping $p_x, p_y \leftrightarrow p_z$). The Coulomb matrix elements $V_{fg}^{\lambda\lambda'}$ include intra-atomic Hubbard repulsions of two holes with opposite spins on one copper and oxygen orbital (U_d, U_p), between different orbitals of copper and oxygen (V_d, V_p), the Hund exchange on copper and oxygen (J_d, J_p), and the nearest-neighbor copper–oxygen Coulomb repulsion V_{pd}.

The GTB method [19] consists in exact diagonalization of the intracell part of p–d Hamiltonian (1)

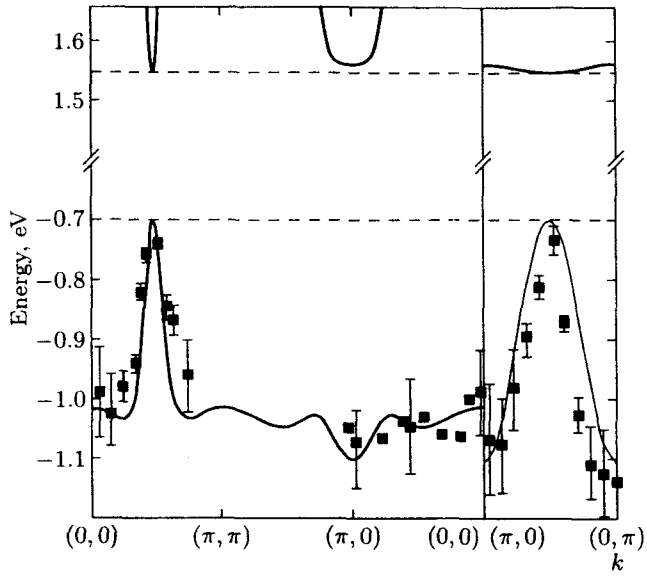

Fig. 1. The GTB method dispersion (doping concentration $x = 0$) of the top of the valence band and the bottom of the conduction band divided by the insulating gap. Horizontal dashed lines mark the in-gap states whose spectral weight is proportional to x. Points with error bars represent experimental ARPES data for $Sr_2CuO_2Cl_2$ [22]

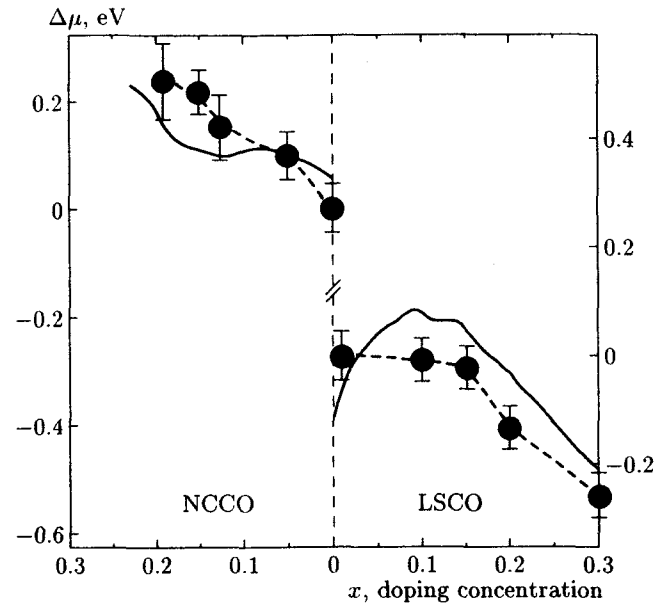

Fig. 2. Dependence of the chemical potential shift $\Delta\mu$ on the doping concentration x for $Nd_{2-x}Sr_xCuO_4$ and $La_{2-x}Sr_xCuO_4$. Straight lines are results of the GTB calculations, filled circles with error bars are experimental points [26]

and perturbative account for the intercell part. For $La_{2-x}Sr_xCuO_4$, the unit cell is the CuO_6 cluster, and the problem of nonorthogonality of the molecular orbitals of adjacent cells is solved explicitly, by constructing the relevant Wannier functions on a five-orbital initial basis of atomic states [20, 21]. In the new symmetric basis, the intracell part of the total Hamiltonian is diagonalized, allowing one to classify all possible effective quasiparticle excitations in the CuO_2-plane according to symmetry.

Calculations [20, 21] of the quasiparticle dispersion and spectral intensities in the framework of the multiband *p–d* model with use of the GTB method are in very good agreement with the ARPES data on insulating compound $Sr_2CuO_2Cl_2$ [22, 23] (see Fig. 1).

Other significant results of this method are as follows [24, 25].

i) Pinning of the Fermi level in $La_{2-x}Sr_xCuO_4$ at low concentrations was obtained in agreement with experiments [27, 26]. This pinning appears due to the in-gap state; the spectral weight of this state is proportional to the doping concentration x, and when the Fermi level comes to this in-gap band, it «stacks» there. In Fig. 2, the doping dependence of the chemical potential shift $\Delta\mu$ for n-type high-T_c $Nd_{2-x}Sr_xCuO_4$ (NCCO) and p-type high-T_c $La_{2-x}Sr_xCuO_4$ (LSCO) is shown. The localized in-gap state also exists in NCCO for the same reason as in LSCO, but its energy is determined by the extremum of the band at the point $(\pi/2, \pi/2)$ and appears to be above the bottom of the conductivity band. Therefore, the first doped electron goes into the band state at $(\pi, 0)$ and the chemical potential merges into the band for a very small concentration. At higher x, it meets the in-gap state with pinning at $0.08 < x < 0.18$ and then μ again moves into the band. The dependence $\mu(x)$ for NCCO is quite asymmetric to the LSCO and also agrees with experimental data [26].

ii) The experimentally observed [28] evolution of the Fermi surface with doping from the hole type (centered at (π, π)) in the underdoped region to the electron type (centered at $(0, 0)$) in the overdoped region is qualitatively reproduced in this method.

iii) The pseudogap feature for $La_{2-x}Sr_xCuO_4$ is obtained as a lowering of the density of states between the in-gap state and the states at the top of the valence band.

The above results were obtained with the following set of the microscopic parameters:

$$\begin{array}{lll} \varepsilon_{d_{x^2-y^2}} = 0, & \varepsilon_{d_{3z^2-r^2}} = 2, & \varepsilon_{p_x} = 1.5, \\ \varepsilon_{p_z} = 0.45, & t_{pd} = 1, & t_{pp} = 0.46, \\ t'_{pd} = 0.58, & t'_{pp} = 0.42, & U_d = V_d = 9, \\ J_d = 1, & J_p = 0, & U_p = V_p = 4, \\ V_{pd} = 1.5. & & \end{array} \quad (2)$$

As the next step, we formulate the effective model. The simplest way to do this is to completely neglect the contribution of the two-particle triplet state $^3B_{1g}$. Then there is only one low-energy two-particle state — the Zhang-Rice-type singlet $^1A_{1g}$, and the effective model is the usual t–J model. But in the multiband p–d model, the difference $\epsilon_T - \epsilon_S$ between the energies of the two-particle singlet and the two-particle triplet depends strongly on various model parameters, particularly on the distance of apical oxygen from planar oxygen, the energy of apical oxygen, the difference between the $d_{3z^2-r^2}$- and $d_{x^2-y^2}$-orbital energies. For realistic values of the model parameters, $\varepsilon_T - \varepsilon_S$ is close to 0.5 eV [21, 32], in contrast to the 3-band model, where this value is about 2 eV (this case was considered in [29, 30]). To take the triplet states into account, we derive the effective Hamiltonian for the multiband p–d model by exclusion of the intersubband hopping between lower (LHB) and upper (UHB) Hubbard subbands, similarly to [12].

The Hubbard X-operator $X_f^{pq} \equiv |p\rangle\langle q|$ on site f represents a natural language to describe strongly correlated electron systems, and we therefore use these operators in the rest of the paper. The X-operators are constructed in the Hilbert space that consists of the vacuum $n_h = 0$ state $|0\rangle$, the single-hole $|\sigma\rangle = \{|\uparrow\rangle, |\downarrow\rangle\}$ state of b_{1g} symmetry, the two-hole singlet state $|S\rangle$ of $^1A_{1g}$ symmetry, and the two-hole triplet state $|TM\rangle$ (where $M = +1, 0, -1$) of $^3B_{1g}$ symmetry.

We write the Hamiltonian as $H = H_0 + H_1$, where the excitations via the charge transfer gap E_{ct} are included in H_1. We then define the operator $H(\epsilon) = H_0 + \epsilon H_1$ and perform the unitary transformation $\tilde{H}(\epsilon) = \exp\left(-i\epsilon\hat{S}\right) H(\epsilon) \exp\left(i\epsilon\hat{S}\right)$. The vanishing of the term linear in ϵ in $\tilde{H}(\epsilon)$ gives the equation for the matrix $\hat{S}$, $H_1 + i\left[H_0, \hat{S}\right] = 0$. The effective Hamiltonian is obtained in the second order in ϵ; at $\epsilon = 1$, it is given by

$$\tilde{H} = H_0 + \frac{1}{2} i \left[H_1, \hat{S}\right]. \quad (3)$$

Thus, for the multiband p–d model (1) in the case of electron doping (n-type systems), we obtain the usual t–J model,

$$H_{t-J} = \sum_{f,\sigma} \varepsilon_1 X_f^{\sigma\sigma} + \sum_{\langle f,g\rangle,\sigma} t_{fg}^{00} X_f^{\sigma 0} X_g^{0\sigma} + \\ + \sum_{\langle f,g\rangle} J_{fg} \left(\mathbf{S}_f \cdot \mathbf{S}_g - \frac{1}{4} n_f n_g\right), \quad (4)$$

where $\mathbf{S}_f$ are spin operators and n_f are the particle number operators. The term $J_{fg} = 2\left(t_{fg}^{0S}\right)^2 / E_{ct}$ is the exchange integral and E_{ct} is the energy of the charge-transfer gap (similar to U in the Hubbard model, $E_{ct} \approx 2$ eV for cuprates). The chemical potential μ is included in ε_1.

For p-type systems, the effective Hamiltonian has the form of a singlet–triplet t–J model [31],

$$H = H_0 + H_t + \sum_{\langle f,g\rangle} J_{fg} \left(\mathbf{S}_f \cdot \mathbf{S}_g - \frac{1}{4} n_f n_g\right), \quad (5)$$

where H_0 (the unperturbed part of the Hamiltonian) and H_t (the kinetic part of H) are given by

$$H_0 = \sum_f \left[\varepsilon_1 \sum_\sigma X_f^{\sigma\sigma} + \varepsilon_{2S} X_f^{SS} + \varepsilon_{2T} \sum_M X_f^{TMTM}\right],$$

$$H_t = \sum_{\langle f,g\rangle,\sigma} \Big\{ t_{fg}^{SS} X_f^{S\bar{\sigma}} X_g^{\bar{\sigma}S} + \\ + t_{fg}^{TT} \left(\sigma\sqrt{2} X_f^{T0\bar{\sigma}} - X_f^{T2\sigma\sigma}\right)\left(\sigma\sqrt{2} X_g^{\bar{\sigma}T0} - X_g^{\sigma T2\sigma}\right) + \\ + t_{fg}^{ST} 2\sigma\gamma_b \left[X_f^{S\bar{\sigma}} \left(\sigma\sqrt{2} X_g^{\bar{\sigma}T0} - X_g^{\sigma T2\sigma}\right) + \text{H.c.}\right] \Big\}.$$

The superscripts of hopping integrals (0,S,T) correspond to excitations that are accompanied by hopping from site f to g, i.e., the Hamiltonian involves the terms $\sum_{\langle f,g\rangle,\sigma} t_{fg}^{MN} X_f^{M\sigma} X_g^{\sigma N}$. The relation between these effective hoppings and microscopic parameters of the multiband p–d model is as follows:

$$\begin{array}{l} t_{fg}^{00} = -2t_{pd}\mu_{fg} 2uv - 2t_{pp}\nu_{fg} v^2, \\ t_{fg}^{SS} = -2t_{pd}\mu_{fg} 2\gamma_x\gamma_b - 2t_{pp}\nu_{fg}\gamma_b^2, \\ t_{fg}^{0S} = -2t_{pd}\mu_{fg}(v\gamma_x + u\gamma_b) - 2t_{pp}\nu_{fg} v\gamma_b, \\ t_{fg}^{TT} = \dfrac{2t_{pd}}{\sqrt{3}}\lambda_{fg} 2\gamma_a\gamma_z + 2t_{pp}\nu_{fg}\gamma_a^2 - 2t'_{pp}\lambda_{fg} 2\gamma_p\gamma_a, \\ t_{fg}^{ST} = \dfrac{2t_{pd}}{\sqrt{3}}\xi_{fg}\gamma_z + 2t_{pp}\lambda_{fg}\gamma_a - 2t'_{pp}\xi_{fg}\gamma_p. \end{array} \quad (6)$$

The factors μ, ν, λ, ξ, χ are the coefficients of the Wannier transformation performed in the GTB method and u, v, γ_a, γ_b, γ_z, γ_p are the matrix elements of the annihilation and creation operators in the Hubbard X-operator representation.

Table 1. Parameters of the effective singlet–triplet model for p-type cuprates obtained in the framework of the GTB method (all values in eV)

ρ	t_ρ^{00}	t_ρ^{SS}	t_ρ^{0S}	t_ρ^{TT}	t_ρ^{ST}	J_ρ
(0,1)	0.373	0.587	−0.479	0.034	0.156	0.115
(1,1)	0.002	−0.050	0.015	−0.011	0	0.0001
(0,2)	0.050	0.090	−0.068	0.015	0.033	0.0023
(2,1)	0.007	0.001	−0.006	−0.004	0.001	0

The resulting Hamiltonian (5) is the generalization of the t–J model to account for the two-particle triplet state. A significant feature of the effective singlet–triplet model is the asymmetry of n- and p-type systems, which is known experimentally. We can therefore conclude that for n-type systems, the usual t–J model is applicable, while for p-type superconductors with complicated structure at the top of the valence band, the singlet–triplet transitions play an important role.

Using the set of microscopic parameters (2) in Table 1, we present numerical values of the hopping and exchange parameters calculated in accordance with (6).

4. COMPARISON OF PARAMETERS

The resulting parameters from *ab initio* [8] and GTB calculations are presented in Table 2. Here, ρ is the connecting vector between two copper centers, t_ρ is the hopping parameter (equal to t_ρ^{SS}, see (5) and (6), in the effective singlet–triplet model), and J_ρ is the antiferromagnetic exchange integral.

As one can see, despite slight differences, the parameters in both methods are very close and show similar dependence on distance. It is worth mentioning that both methods give disproportionality between t_ρ and J_ρ. In the usual t–J model, the proportionality $J_\rho = 2t_\rho^2/U$ occurs as soon as this t–J model is obtained from the Hubbard model with the Hubbard repulsion U. In the singlet–triplet model, the intersubband hopping t_ρ^{0S} that determines the value of J_ρ is different from the intrasubband hopping t_ρ^{SS} that determines t_ρ. This leads to a more complicated relation between t_ρ and J_ρ.

Table 2. Comparison of *ab initio* parameters [8] and parameters obtained in the framework of the GTB method (all values in eV)

	ab initio		GTB method	
ρ	t_ρ	J_ρ	t_ρ	J_ρ
(0,1)	0.486	0.109	0.587	0.115
(1,1)	−0.086	0.016	−0.050	0.0001
(0,2)	−0.006	0	0.090	0.0023
(2,1)	0	0	0.001	0

In the framework of the LDA band structure of YBa_2CuO_{7+x} and within the orbital projection approach, it was shown [33] that the 1-band Hamiltonian reduced from the eight-band Hamiltonian should include not only the nearest-neighbor hopping terms (t), but also second (t') and third (t'') nearest-neighbor hoppings. In the GTB method, the dependence of the hoppings t_ρ on distance automatically results from the distance dependence of the coefficients of the Wannier transformation performed in this method (see Eq. (6)). To show the correspondence between the results of different authors, we compare our parameters and the parameters widely used by different groups in Table 3.

The parameters extracted from experimental data are listed in columns I–VI of Table 3. The LDA calculated parameters are presented in columns VII and VIII. Our results for hoppings agree best with columns III, VII, and VIII. This similarity is not surprising. In the LDA calculations, the bandwidth of strongly correlated electron systems is usually overestimated because the strong Coulomb repulsion of electrons is not taken into account properly. But it is well known that the Fermi surface obtained by this method is in very good agreement with experiments. The main contribution to the shape of the Fermi surface comes from kinetic energy of the electrons (hopping parameters), and therefore the values of hoppings should be properly estimated by the LDA calculations (columns VII, VIII). In [37, 38] (column III), the parameters were obtained by fitting the LSCO tight-binding Fermi sur-

Table 3. Comparison of the calculated parameters and parameters used in the literature

quantity	0[a] LSCO here	0[b] LSCO here	I[c] LSCO [34]	II[c] LSCO [35, 36]	III[c] LSCO [37, 38]	IV[c] Bi2212 SCOC [37, 38, 39]	V[c] YBCO [40]	VI[c] SCOC [41]	VII[d] YBCO [33]	VIII[d] LSCO [42]	IX[e] LSCO [43]	X[e] YBCO [43]
t, eV	0.587	0.486	0.416	0.35	0.35	0.35	0.40	0.40	0.349	0.43	–	–
t'/t	−0.085	−0.18	−0.350	−0.20	−0.12	−0.34	−0.42	−0.35	−0.028	−0.17	–	–
t''/t	0.154	0.012	–	0.15	0.08	0.23	−0.25	0.25	0.178	–	–	–
J, eV	0.115	0.109	0.125	0.14	0.14	0.14	0.17	0.12	–	–	0.126	0.125, 0.150
$J/\|t\|$	0.196	0.224	0.300	0.40	0.40	0.40	0.43	0.30	–	–	–	–

[a] GTB method parameters,
[b] *ab initio* parameters obtained in the present paper,
[c] parameters obtained by fitting to experimental data,
[d] *ab initio* parameters,
[e] parameters obtained from two-magnon Raman scattering.

face to the experimental one. This procedure should give the same values as the LDA calculation and, as one can see, it does. By the same technique, the parameters for $Bi_2Sr_2CaCu_2O_{8+x}$ (Bi2212, column IV) were obtained [37, 38]. These parameters are different from those in the LSCO case and in the present paper; the most straightforward explanation is a more complicated structure of the Fermi surface of Bi2212 compound. In the present paper, single-layer (LSCO-like) compounds are considered and the effects of multiple CuO_2-planes (i.e., bilayer splitting) are neglected. The difference between our hoppings and hoppings in column V appears due to the same reason (in Ref. [40], the $YBa_2Cu_3O_6$ insulating compound was investigated).

In the last two columns of Table 3, the antiferromagnetic exchange parameters J obtained from the two-magnon Raman scattering analysis by momentum expansion (LSCO, column IX) and spin-wave theory (YBCO, column X) are presented (for details, see review [43] and references therein). Our values of J (column 0) are in good agreement with the values extracted from experiments and similar to those listed in columns I–VI.

In [44], the Heisenberg Hamiltonian on the square lattice with plaquette ring exchange was investigated. The fitted exchange interactions $J = 0.151$ eV, $J' = J'' = 0.025J$ give the values for the spin stiffness and the Neel temperature in excellent agreement with experimental data for insulating compound La_2CuO_4. In the GTB calculations, $J = 0.115$ eV, $J' = 0.0009J$, and $J'' = 0.034J$. The values of J are close to each other, but different. This difference could be explained by the fact that authors of [44] used the Heisenberg Hamiltonian and inclusion of the hopping term should renormalize the presented exchange interaction values. Agreement between J'' in the GTB calculations and in Ref. [44] is good but the values of J' are completely different. The last issue could be attributed to oversimplification of calculations in [44], where the authors put $J' = J''$ by hand to restrict the number of fitting parameters.

We now discuss the difference between our parameters and the parameters in columns I, II, VI, and column IV (SCOC). The hoppings in the papers cited above were obtained by fitting the t–t'–t''–J model dispersion to the experimental ARPES spectra [22, 39] for insulating $Sr_2CuO_2Cl_2$. We claim that the discrepancy between the GTB method results and the t–t'–t''–J model results stems from the absence of singlet–triplet hybridization in the latter model. This statement can be proved by comparing the dispersion in the «bare» t–t'–J model (4) and in the singlet–triplet t–t'–J model (5). The paramagnetic nonsuperconducting phase was investigated in the Hubbard-I approximation in both the singlet–triplet and $t - t' - J$ models. The results for optimal doping (with the concentration of holes $x = 0.15$) are presented in Fig. 3.

There is a strong mixture of singlet and triplet bands along the $(0,0) - (\pi,\pi)$ and $(\pi,0) - (0,0)$ directions due to the t^{ST} matrix element (see (6)) in both paramagnetic (Fig. 3) and antiferromagnetic phases (Fig. 1). It is exactly the admixture of the triplet states

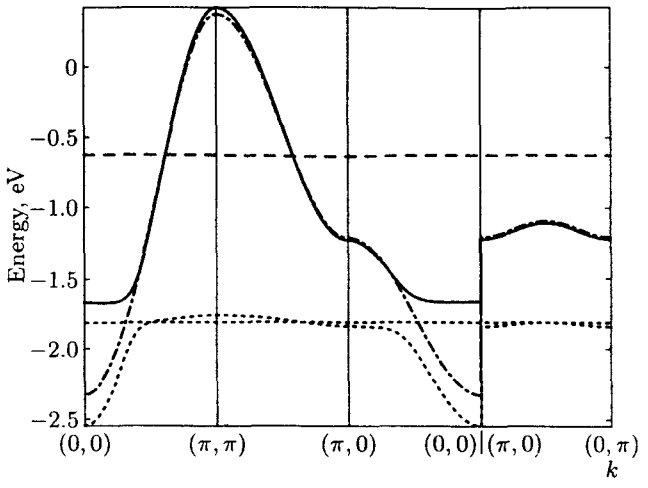

Fig. 3. Dispersion curves on top of the valence band for the effective singlet–triplet model (singlet subband is shown with the solid line, triplet subbands with dotted lines) and the t–t'–J model (the dash-dotted line) at the optimal doping $x = 0.15$; the dashed line represents the self-consistently obtained chemical potential μ

that determines coincidence of the dispersion in our approach and the ARPES data in the undoped SCOC at the energies 0.3–0.4 eV below the top of the valence band, where the t–t'–J model [34] fails and the t–t'–t''–J model involves the additional parameter t'' [35, 37]. In our approach, this parameter is not as necessary as in the «bare» t–t'–J model, because the singlet–triplet hybridization is included explicitly.

In Ref. [45], the t–t'–t''–J model was also used to describe the dispersion of insulating $Sr_2CuO_2Cl_2$, with the same set of parameters as in Refs. [37, 38]. But the authors of Ref. [45] used a totally different definition of hopping parameters: in their paper, the t' term stands for hopping between two nearest-neighbor oxygens and the t'' term stands for the hopping between two oxygens on the two sides of Cu. Such a definition is completely different from that used in other cited papers, where t, t', t'' terms stands for hoppings between plaquettes centered on copper sides, and we cannot therefore make comparison with their results.

The analysis of the data in Table 3 gives the following ranges for different parameters: $0.350 \div 0.587$ eV for t, $-0.420 \div -0.028$ for t'/t, $0.012 \div 0.250$ for t''/t with the exception of the value in Ref. [40], and $0.115 \div 0.150$ eV for J. In general, we see a close similarity in the first-neighbor hopping t and the interaction J for the different methods and materials, and more discrepancy in subtle parameters as such t' and t''.

5. CONCLUSION

One of the significant results in this paper is the relation (6) between microscopic parameters and parameters of the effective singlet–triplet model. The effective model parameters are therefore not free any more and have a direct physical meaning coming from the dependence on microscopic parameters. The parameters of the effective singlet–triplet model were obtained from both *ab initio* and model calculations. Model calculations were performed in the framework of the GTB method for insulating single-layer copper oxide superconductor. The *ab initio* calculations for La_2CuO_4 were done by the conventional LDA TB-LMTO method. The agreement between the parameters is remarkably good. The obtained parameters are also in good agreement with widely used parameters of the t–t'–t''–J model, although some difference exists. This difference is attributed to the neglect of triplet excitations in the simple t–t'–t''–J model. After careful analysis, we proposed the set of parameters for effective models (e.g., the t–t'–t''–J model or the effective singlet–triplet model) for proper quantitative description of physics of hole-doped high-T_c cuprates.

M. M. K., V. A. G., and S. G. O. thank the Free University of Berlin for hospitality during their stay. This work was supported by the INTAS (Grant 01-0654), Joint Integration Program of Siberian and Ural Branches of the Russian Academy of Science, Russian Foundation for Basic Research (Grant 03-02-16124), Russian Federal Program «Integratsia» (Grant B0017), Program Physical Branch of the Russian Academy of Science «Strongly Correlated Electron Systems», and Siberian Branch of Russian Academy of Science (Lavrent'yev Contest for Youth Scientists), RFFI 04-02-16096 (VIA, IAN, MAK, ZVP), RFFI 03-02-39024 (VIA, MAK, IAN), Grant of the President of the Russian Federation for young scientists MK-95.2003.02 (IAN), the Dynasty Foundation and ICFPM (IAN, MMK), Russian Science Support Foundation program for young PhD of Russian Academy of Science 2004 (IAN).

REFERENCES

1. Z.-X. Shen and D. S. Dessau, Phys. Rep. **253**, 1 (1995); E. Dagotto, Rev. Mod. Phys. **66**, 763 (1994); A. P. Kampf, Phys. Rep. **249**, 219 (1994).

2. V. J. Emery, Phys. Rev. Lett. **58**, 2794 (1987).

3. C. M. Varma et al., Sol. St. Commun. **62**, 681 (1987).
4. Yu. Gaididei and V. Loktev, Phys. St. Sol. B **147**, 307 (1988).
5. O. K. Andersen and O. Jepsen, Phys. Rev. Lett. **53**, 2571 (1984).
6. O. K. Andersen, Z. Pawlowska, and O. Jepsen, Phys. Rev. B **34**, 5253 (1986).
7. J. D. Axe and M. K. Crawford, J. Low Temp. Phys. 95, **271** (1994).
8. V. I. Anisimov et al., Phys. Rev. **66**, 100502 (2002).
9. A. I. Lichtenstein et al., J. Magn. Mag. Matter **67**, 65 (1987); A. I. Lichtenstein, V. I. Anisimov, and J. Zaanen, Phys. Rev. B **52**, R5467 (1995).
10. V. I. Anisimov, J. Zaanen, and O. Andersen, Phys. Rev. B **44**, 943 (1991); V. I. Anisimov et al., J. Phys.: Condens. Matter **9**, 767 (1997).
11. O. Gunnarsson et al., Phys. Rev. B **39**, 1708 (1989); V. I. Anisimov and O. Gunnarsson, Phys. Rev. **43**, 7570 (1991).
12. K. A. Chao, J. Spalek, and A. M. Oles, J. Phys. C: Sol. Stat. Phys. **10**, 271 (1977).
13. J. C. Hubbard, Proc. Roy. Soc. A **276**, 238 (1963).
14. M. S. Hybertsen, M. Schluter, and N. E. Christensen, Phys. Rev. B **39**, 9028 (1989).
15. A. K. McMahan, J. F. Annett, and R. M. Martin, Phys. Rev. B **42**, 6268 (1990).
16. A. Bianconi et al., Phys. Rev. B **38**, 7196 (1988).
17. H. Romberg et al., Phys. Rev. B **41**, 2609 (1990).
18. C. H. Chen et al., Phys. Rev. Lett. **68**, 2543 (1992).
19. S. G. Ovchinnicov and I. S. Sandalov, Physica C **161**, 607 (1989).
20. V. A. Gavrichkov et al., Phys. Rev. B **64**, 235124 (2001).
21. V. A. Gavrichkov et al., Zh. Eksp. Teor. Fiz. **118**, 422 (2000).
22. B. O. Wells et al., Phys. Rev. Lett. **74**, 964 (1995).
23. C. Dürr et al., Phys. Rev. B **63**, 014505 (2000).
24. A. A. Borisov, V. A. Gavrichkov, and S. G. Ovchinnikov, Mod. Phys. Lett. B **17**, 479 (2003).
25. A. A. Borisov, V. A. Gavrichkov, and S. G. Ovchinnikov, Zh. Eksp. Teor. Fiz. **124**, 862 (2003).
26. N. Harima et al., Phys. Rev. B **64**, 220507(R) (2001).
27. A. Ino et al., Phys. Rev. Lett. **79**, 2101 (1997).
28. A. Ino et al., Phys. Rev. B **65**, 094504 (2002).
29. J. Zaanen, A. M. Oles, and P. Horsch, Phys. Rev. B **46**, 5798 (1992).
30. R. Hayn et al., Phys. Rev. B **47**, 5253 (1993).
31. M. Korshunov and S. Ovchinnikov, Fiz. Tv. Tela **43**, 399 (2001).
32. R. Raimondi et al., Phys. Rev. B **53**, 8774 (1996).
33. O. K. Andersen et al., J. Phys. Chem. Sol. **56**, 1573 (1995).
34. A. Nazarenko et al., Phys. Rev. B **51**, 8676 (1995).
35. V. I. Belinicher, A. I. Chernyshev, and V. A. Shubin, Phys. Rev. B **53**, 335 (1996).
36. V. I. Belinicher, A. I. Chernyshev, and V. A. Shubin, Phys. Rev. B **54**, 14914 (1996).
37. T. Tohayama and S. Maekawa, Supercond. Sci. Technol. **13**, R17 (2000).
38. T. Tohayama and S. Maekawa, Phys. Rev. B **67**, 092509 (2003).
39. C. Kim et al., Phys. Rev. Lett. **80**, 4245 (1998).
40. F. P. Onufrieva, V. P. Kushnir, and B. P. Toperverg, Phys. Rev. B **50**, 12935 (1994).
41. R. Eder, Y. Ohta, and G. A. Sawatzky, Phys. Rev. B **55**, R3414 (1997).
42. E. Pavarini et al., Phys. Rev. Lett. **87**, 047003 (2001).
43. W. Brenig, Phys. Rep. **251**, 153 (1995).
44. A. A. Katanin and A. P. Kampf, Phys. Rev. B **66**, 100403(R) (2003).
45. T. Xiang and J. M. Wheatley, Phys. Rev. B **54**, R12653 (1996).